Demonstration of Ultraviolet μLED Array With Novel Electrical Contact Etch Mask

Matthew Seitz, *Graduate Student Member, IEEE*, Matthew Hartensveld, *Member, IEEE*, Bryan Melanson, *Graduate Student Member, IEEE*, Jacob Boisvere, and Jing Zhang, *Member, IEEE*

***Abstract*— We report on the realization of a uniform array of electrically driven, individually addressable micro light-emitting diodes (μLEDs) with diameters of 2.5 μm emitting at 372 nm. This highly ordered array was fabricated via a top-down fabrication approach using a novel Ni/Au/Ni structure which combines both a Ni/Au low-resistance electrical contact and durable Ni etch mask. The use of this novel structure allows individual μLEDs to be addressed with promising electroluminescence intensity and narrow linewidth at ultraviolet-A (UV-A) band. This improved control over μLED output power and emission location makes our approach an important step towards the development of high efficiency UV-A μLEDs for a range of applications.**

***Index Terms*— Electrical contact, GaN, micropillar, ultraviolet LED.**

I. Introduction

ULTRAVIOLET (UV) light has numerous applications in sterilization and disinfection, [1], [2] curing of polymers, resins, inks for 3D printing, [3], [4] spectroscopy and non-destructive testing, [5] and shows promise for high-speed optical communication [6] and displays [7]. Still further applications have been identified as materials and fabrication advances enable emission of shorter wavelengths, [8] higher efficiencies, [9], [10] and smaller devices [11]. Within the UV spectrum, UV-A light, with a wavelength between 315-400 nm, is of especially high interest for photolithography [12] and as a photocatalyst for air and water treatment [7], [8]. Conventional UV-A light emitting diodes (LEDs) based on mesa structures typically have a low overall efficiency, caused in part by especially low light extraction efficiency, typically between 10% - 40% [3]. The poor light extraction efficiency can be improved by shrinking the commonly used mesa structures to micropillars and nanowires, [15] thus μLEDs are of great interest.

Micropillar and nanowire gallium nitride (GaN) structures can be fabricated either through bottom-up or top-down processes. Selective area epitaxy (SAE) can be used to grow micropillar and nanowire structures from a patterned template in a bottom-up fabrication process [16]. However, this approach only offers limited control over the growth rate, diameter, and length of the resulting structures [17]. As an alternative, structures can be instead formed through a top-down approach. In this case, crystal growth is performed at the full wafer scale and structures are formed through photolithography and reactive ion etching (RIE) [18]. This fabrication approach uses well established processes produces highly uniform structures with precise control over their placement and spacing.

Though our previous works have demonstrated successful top-down fabrication of micropillar and nanowire GaN LEDs [18], [19], [20], [21], [22], [23], another limiting factor for high-efficiency UV μLEDs is poor p-type doping of GaN. Magnesium can be incorporated as a p-type dopant during epitaxial growth, but it forms electrically-inactive complexes with hydrogen [24] and must be activated after growth, typically through high temperature annealing [25]. This activation process is highly inefficient, with only up to 5.25% activation [26] due to magnesium's high activation energy [27]. This poor doping efficiency leads to an extremely high p-GaN work function, predicted to be 6.6 eV, higher than that of all pure metals [28]. The issue of high p-GaN work function has led to the development and optimization of alloyed or multi-layer metal contacts, such as commonly used nickel (Ni)/gold (Au) in an attempt to minimize the Schottky barrier height at the metal-semiconductor interface and form a low-resistance, ohmic electrical contact [29].

The use of nanowire and micropillar structures has been shown to improve both the quantum efficiency and optical output power of the device [30]. As research investigates ever smaller devices, existing fabrication processes become steadily less applicable. Fabrication of GaN LEDs typically consists of deposition and patterning of an etch mask, RIE to form the mesa structure, post-etch removal of the etch mask, and finally, deposition of p-type electrical contacts [21], [31]. However, this well demonstrated process becomes increasingly challenging to implement for ever shrinking devices. The extremely precise lithographic alignment necessary to accurately produce these electrical contacts post-etching presents significant challenges and necessitates a new approach. Previous works [21], [32], [33], [34] use a single, common electrical contact to avoid this challenge. However, this prevents the possibility of individual control of single μLEDs.

In this work, we propose a novel solution to these challenges and demonstrate the successful fabrication of an array of individually addressable 2.5 μm diameter UV μLEDs emitting at 372 nm. Our proposed 20 nm Ni/20 nm Au/200 nm Ni

Manuscript received 18 April 2023; revised 7 July 2023 and 21 August 2023; accepted 27 August 2023. Date of publication 1 September 2023; date of current version 21 September 2023. This work was supported in part by the National Science Foundation under Award ECCS 1751675. *(Corresponding authors: Matthew Seitz; Jing Zhang.)*

Matthew Seitz, Bryan Melanson, Jacob Boisvere, and Jing Zhang are with the Electrical and Microelectronic Engineering Department, Rochester Institute of Technology, Rochester, NY 14623 USA (e-mail: ms3897@rit.edu; jzeme@rit.edu).

Matthew Hartensveld is with Innovation Semiconductor Inc., Rochester, NY 14604 USA.

Color versions of one or more figures in this article are available at https://doi.org/10.1109/JQE.2023.3310968.

Digital Object Identifier 10.1109/JQE.2023.3310968

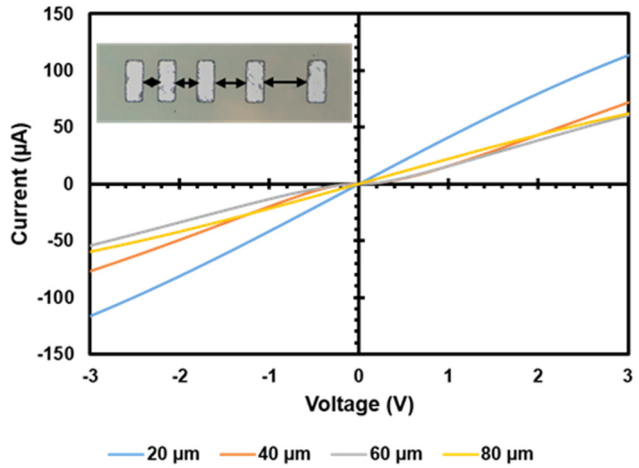

Fig. 1. I-V characteristics from 20 nm Ni/20 nm Au/200 nm Ni TLM measurements after annealing with spacings of 20 μm, 40 μm, 60 μm, and 80 μm between pads. Inset: microscope image of TLM structures used for testing, with spacing indicated by double arrows.

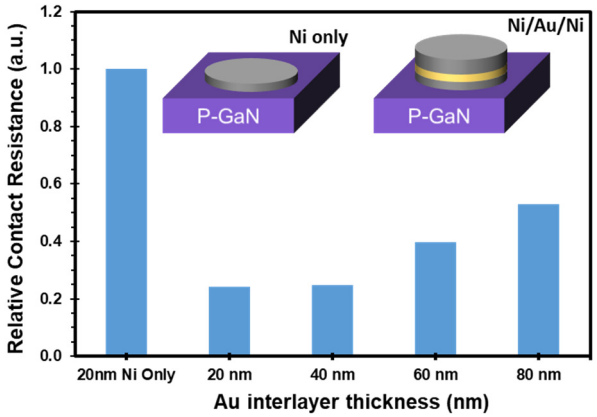

Fig. 2. Relative contact resistance comparison of annealed single layer Ni contact and three-layer Ni/Au/Ni contacts with varying Au interlayer thicknesses.

metal structure serves to both act as the durable plasma etch mask necessary for the fabrication of high aspect ratio devices and as a low resistance electrical contact for fabricated devices. By pre-depositing the electrical contacts for each device, the need for a universal, common electrical contact is eliminated and individual UV μLEDs within the array can be driven independently of the rest of the array, offering greater control over the emitters. This novel fabrication approach offers several advantages over existing processes, most notably enabling the fabrication of individually-addressable micropillar and nanowire LED devices and arrays.

II. Contact Structure Optimization and Device Fabrication

Our initial optimization of the p-type metal contact stack for our UV-A μLEDs was performed through a series of transfer length method (TLM) experiments. These initial experiments used a contact metal stack consisting of 20 nm of Ni and an Au interlayer of 20 nm, 40 nm, 60 nm, or 80 nm, to serve as the ohmic contact, followed by a 200 nm of Ni to serve as the durable etch mask for the chlorine-based plasma etch. All metals were deposited via thermal evaporation onto the surface of the top p-GaN layer, doped to a level of $\sim 10^{18}/cm^3$ with Mg, forming a set of 30 μm x 100 μm contact pads spaced 20 μm, 40 μm, 60 μm, and 80 μm apart, as shown in the inset of Figure 1. Following metal evaporation, samples were transferred to a rapid thermal annealing (RTA) tool and were annealed for 5 minutes at 500°C in an oxygen environment. A second set of similar TLM contacts, consisting of a single 20 nm Ni layer deposited onto p-GaN, were also deposited to serve as a reference, and were also annealed for 5 minutes at 500°C in an oxygen environment. TLM measurements were then performed and the electrical performance of the Ni/Au/Ni contacts was compared to that of the single layer Ni control contact structures. As shown in Figure 2, the use of a Ni/Au/Ni contact structure resulted in a reduction of contact resistance of up to 75% when compared to contacts composed solely of Ni. For a simple Ni/Au bilayer contact, annealing in an oxygen-containing atmosphere causes outdiffusion and oxidation of Ni. This results in the formation of a discontinuous Au layer, interrupted by NiO islands at the GaN surface. The presence of NiO, a p-type semiconductor itself, at the GaN-metal interface serves to reduce the overall contact resistance. Additionally, further interdiffusion at the surface leads to the formation of an Au-Ga solid solution and thus acceptor-like Ga vacancies at the GaN-metal interface, further reducing contact resistance. This process of interdiffusion and oxidation progresses differently with the addition of a Ni capping layer, as with our novel contact structure. Exposed Ni metal quickly oxidizes during annealing, as with the Ni/Au contact. However, unlike the bilayer Ni/Au contact, the thick Ni capping layer and increasing Au interlayer thickness slows the formation or transport of NiO to the GaN-metal interface. The presence of un-oxidized Ni in contact with the p-GaN surface, detrimental to the formation of a low-resistance, ohmic contact. This can be seen in Figure 2 as an increase in measured contact resistance with increasing Au interlayer thickness [35], [36], [37]. Based on this initial optimization, an Au interlayer thickness of 20-40 nm showed the lowest contact resistance. After annealing, these Ni/Au/Ni electrical contacts showed nearly linear current-voltage (I-V) characteristics for all different spacing lengths, as shown in Figure 1. Based on these TLM results, an Au thickness of 20 nm was selected for subsequent μLED fabrications.

Fabrication of the UV-A μLED array was performed on a c-plane epitaxial stack similar to that used by Huang, [38] which consisted of a 20 nm AlN buffer layer, a 2 μm undoped GaN layer, a 2.5 μm n-AlGaN lower cladding layer, an InGaN/AlGaN active region, a 15 nm p-AlGaN upper cladding layer, and a 200 nm p-GaN contact layer, as shown in Figure 3(a). The active region consisted of 10 periods of 3 nm $In_{0.03}Ga_{0.97}N$ wells and 11 nm $Al_{0.02}Ga_{0.98}N$ barriers. The epitaxial structure was grown on a sapphire substrate using metalorganic chemical vapor deposition (MOCVD). As shown in Figure 3(b), to fabricate devices, lift-off resist (LOR) and photoresist were deposited and patterned using 405 nm direct write lithography using a Heidelberg DWL 66+,

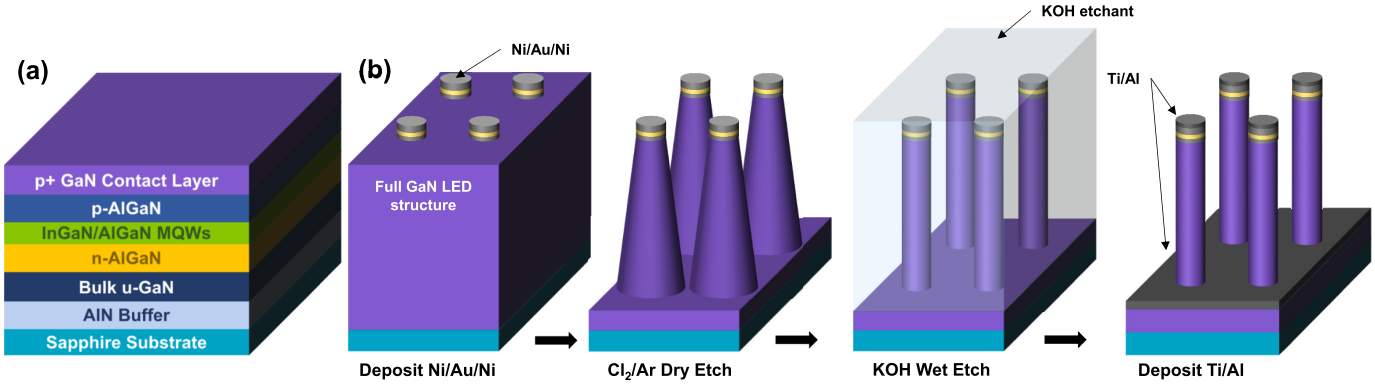

Fig. 3. (a) GaN UV LED epitaxial structure. (b) Device fabrication process showing deposition of Ni/Au/Ni contact and etch mask, Cl2/Ar dry etching, wet etching in KOH solution, and final deposition of Ti/Al electrical contacts.

and the metal stack was deposited using highly anisotropic thermal evaporation. Based on prior TLM results, Ni/Au/Ni thicknesses of 20/20/200 nm were utilized. After metal lift-off, dry etch was performed using a Cl_2/Ar plasma (40/10 sccms Cl_2/Ar, 500 W inductively coupled plasma (ICP) power, 225 W forward power, 440 nm/min etch rate, 192 second duration) in a PlasmaTherm ICP-RIE to form a large array of 2.5 μm diameter, 1.4 μm tall micropillars with a 10 μm pitch, as shown in Figure 4(a). The sidewalls of these micropillars are left roughened, as shown in Figure 4(b), indicative of surface damage typically caused by the ICP-RIE etch process [39]. Hydroxyl-based chemistries, such as KOH, are commonly used on GaN structures to passivate and to remove surface damage caused by dry etching [22]. The wafer was submerged in a solution of 40% AZ400K (a photoresist developer containing 2 wt% KOH) heated to 80°C for a total of 15 minutes. To ensure that this etch duration was sufficient to produce highly vertical sidewalls, the wafer was examined and imaged using a scanning electron microscope (SEM), shown in Figure 4(c). Following this inspection, the p-type metal was annealed at 450°C for 40 seconds under nitrogen. A universal n-type contact was then deposited using thermal evaporation. The deposition of the n-contact was self-aligned in that the micropillars themselves were used to mask deposition of the n-metal on the sidewalls of the micropillars. The sample was carefully aligned directly above the evaporation source, and the highly anisotropic nature of thermal evaporation allowed metal deposition to occur on the tops of the micropillars and on the n-AlGaN at the bases of the micropillars, but not on the micropillar sidewalls. This n-metal stack consisted of 40/200 nm Ti/Al. After this deposition, the LED array was completed and the individually addressable UV-A μLEDs could be tested and characterized.

III. Electrical and Optical Characterizations of μLEDs

Electrical testing of individual μLEDs was performed by manually probing the n- and p-contacts and applying a forward bias. These tests show a turn on voltage of approximately 5 V, as shown in Figure 5, above this threshold voltage, individual μLEDs illuminate as shown in the inset of Figure 5. By placing an optical fiber near the probed device, electroluminescence (EL) spectra can be collected. These spectra show a peak emission wavelength of 372 nm, as shown in Figure 6. Emission peaks show a consistent FWHM of approximately 11 nm, similar to what is reported in other works [40], [41], [42]. As drive current is increased from 60 μA to 150 μA, we observe both an increase in EL intensity and a slight redshift of approximately 2 nm in peak emission wavelength. This redshift is expected and is likely due to an increase in junction temperature with increasing drive current [42].

We have also analyzed light extraction efficiency from UV-A μLEDs with three-dimensional (3D) finite-difference time-domain (FDTD) simulations using commercially available Synopsys Fullwave software which is specifically designed to model light propagation in a range of structures. These simulations model the propagation of electromagnetic waves through a defined structure by finding direct solutions for Maxwell's curl equations. Simulations were conducted using methods similar to those used in Ref. [20].

Simulation setup begins with modelling of the structure of interest, a 2.5 μm diameter, 1.4 μm tall μLED. Material types and properties can be defined for the different layers within the structure and our modeled μLED uses a similar layer structure as our fabricated μLEDs, shown in Figure 3(a). Three dipole sources were placed at the center of the MQW region, aligned with the x, y, and z-axes and a 20 nm cubic monitor was defined encompassing these dipole sources to capture the full luminous flux. This flux is compared against the luminous flux measured by another set of monitoring planes placed outside the simulated μLED. These exterior planes form a rectangular prism, extending 500 nm beyond the sides and top of the μLED structure and extending 200 nm below the bottom nAlGaN surface. The external monitor planes act as perfect absorbers, preventing unintended wave reflections off the simulation boundaries. Overall light extraction efficiency (LEE) can then be calculated as the ratio of flux measured by the external monitor planes around the sidewalls and top μLED surface and the total flux produced by the combined dipole sources in the MQW region.

Two sets of simulations were conducted, one with a simple, single 20 nm layer of Ni covering the top surface of the

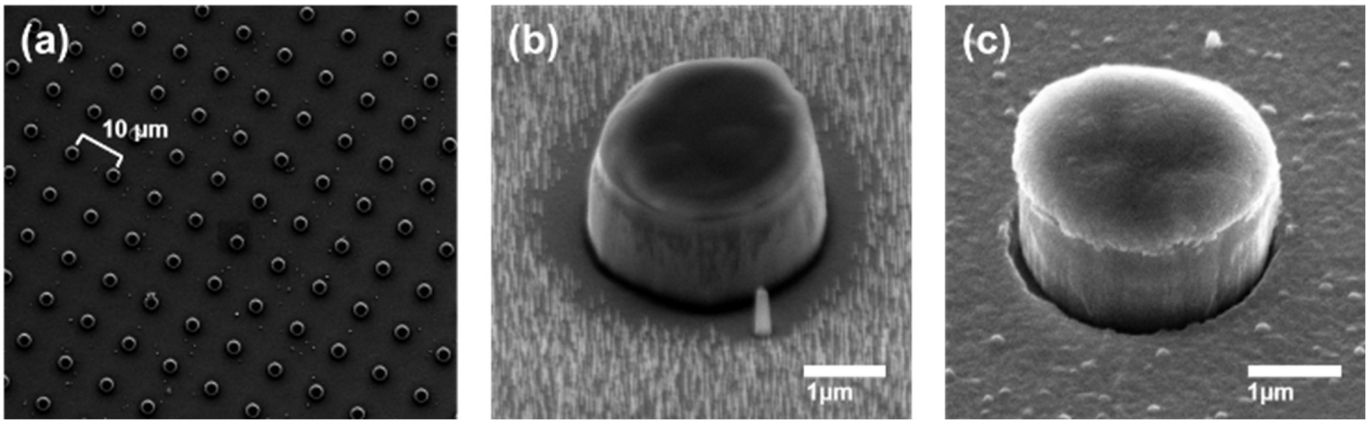

Fig. 4. SEM images of (a) fabricated ordered UV-A μLED array, (b) micropillar with flared base after dry etching, (c) μLED after follow-up wet etching and n-metal deposition.

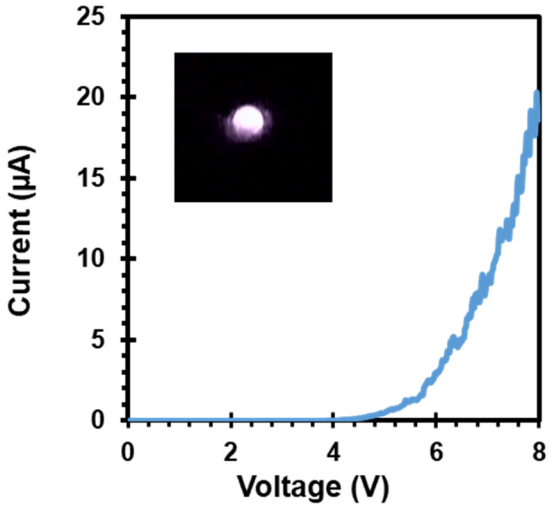

Fig. 5. I-V characteristics from a single UV-A μLED. Inset: microscope image of one illuminated UV-A μLED.

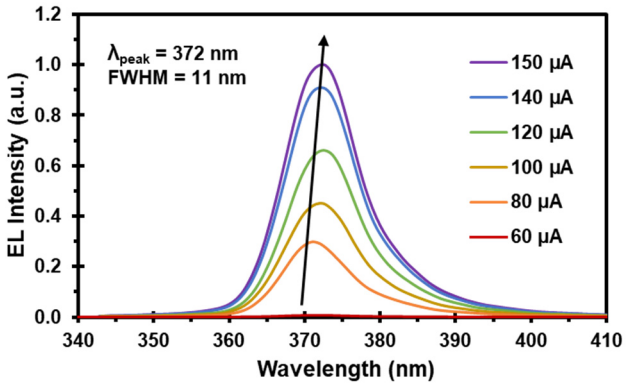

Fig. 6. EL spectra recorded from a single μLED under different drive currents.

μLED that represents common p-contact cases, and another using our novel 20 nm Ni/20 nm Au/200 nm Ni contact structure covering the μLED top surface. Simulated electric field intensity within the two μLED structures can be seen in Figure 7. These simulation results indicate that even in the case of a thin 20 nm layer of Ni covering the top surface,

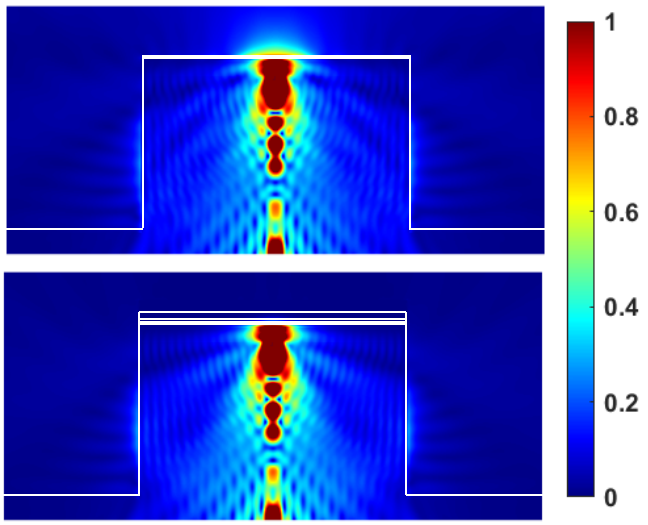

Fig. 7. Simulated electric field intensity within μLEDs, (top) with a 20 nm Ni contact deposited on the top surface, and (bottom) with a 20 nm Ni/20 nm Au/200 nm Ni contact deposited on the top surface.

extraction efficiency is only 1.6% through the top surface with the majority of escaping light being emitted instead through the sidewalls. When our novel Ni/Au/Ni structure is simulated, the additional metal layers have a negligible effect on total light extraction from the whole μLED structure, calculated to be 25.8% for the Ni top contact and 24.2% for the Ni/Au/Ni contact. Overall, these results suggest that the use of a Ni/Au/Ni contact structure offers several advantages in terms of fabrication and electrical contact resistance without significantly affecting total light extraction from the device.

IV. Conclusion

In conclusion, we have successfully demonstrated an array of individually addressable UV-A GaN μLEDs emitting at 372 nm. These μLEDs were fabricated using a novel Ni/Au/Ni structure to form highly uniform 2.5 μm diameter, 1.4 μm tall μLEDs with a 10 μm pitch. This novel Ni/Au/Ni structure serves as both a durable dry etch mask during device fabrication and as a low resistance electrical contact during

device operation, allowing individual μLEDs to be probed and tested. Electrical testing of these μLEDs shows a consistent, narrow linewidth of 11 nm and a turn on voltage of 5 V. This novel approach enables an extremely high level of control over the output of μLED arrays as individual devices can be driven rather than the whole array. Additional study of this process could further improve the effectiveness of this Ni/Au/Ni structure by minimizing the capping Ni layer thickness based on the desired etch depth, potentially lowering device turn on voltages. Overall device efficiency could also be improved through additional optimization of the annealing process to further reduce contact resistance. By controlling individual μLEDs, total emission power and the location of light generation can be easily varied making this a promising approach for numerous applications including photolithography and photocatalytic processes. This approach can also be applied to μLEDs emitting at other wavelengths, including visible light, which can open the door for higher resolution displays.

REFERENCES

[1] K. Oguma, R. Kita, H. Sakai, M. Murakami, and S. Takizawa, "Application of UV light emitting diodes to batch and flow-through water disinfection systems," *Desalination*, vol. 328, pp. 24–30, Nov. 2013, doi: 10.1016/j.desal.2013.08.014.

[2] M. P. Akgün and S. Ünlütürk, "Effects of ultraviolet light emitting diodes (LEDs) on microbial and enzyme inactivation of apple juice," *Int. J. Food Microbiol.*, vol. 260, pp. 65–74, Nov. 2017, doi: 10.1016/j.ijfoodmicro.2017.08.007.

[3] C. Dreyer and F. Mildner, "Application of LEDs for UV-curing," in *III-Nitride Ultraviolet Emitters* (Springer Series in Materials Science), vol. 227, M. Kneissl J. Rass, Eds. Cham, Switzerland: Springer, 2016, pp. 415–434, doi: 10.1007/978-3-319-24100-5_15.

[4] R. Ding, Y. Du, R. B. Goncalves, L. F. Francis, and T. M. Reineke, "Sustainable near UV-curable acrylates based on natural phenolics for stereolithography 3D printing," *Polym. Chem.*, vol. 10, no. 9, pp. 1067–1077, Feb. 2019, doi: 10.1039/C8PY01652F.

[5] K. Włodarska, J. Szulc, I. Khmelinskii, and E. Sikorska, "Non-destructive determination of strawberry fruit and juice quality parameters using ultraviolet, visible, and near-infrared spectroscopy," *J. Sci. Food Agricult.*, vol. 99, no. 13, pp. 5953–5961, Oct. 2019, doi: 10.1002/jsfa.9870.

[6] M. H. Memon et al., "Quantum dots integrated deep-ultraviolet micro-LED array toward solar-blind and visible light dual-band optical communication," *IEEE Electron Device Lett.*, vol. 44, no. 3, pp. 472–475, Mar. 2023, doi: 10.1109/LED.2023.3239393.

[7] M.-C. Wu and I.-T. Chen, "High-resolution 960 × 540 and 1920 × 1080 UV micro light-emitting diode displays with the application of maskless photolithography," *Adv. Photon. Res.*, vol. 2, no. 7, Jul. 2021, Art. no. 2100064, doi: 10.1002/adpr.202100064.

[8] C. Zhang, K. Jiang, X. Sun, and D. Li, "Recent progress on AlGaN based deep ultraviolet light-emitting diodes below 250 nm," *Crystals*, vol. 12, no. 12, p. 1812, Dec. 2022, doi: 10.3390/cryst12121812.

[9] Q. Dai, X. Zhang, Z. Wu, X. Zeng, and S. Wang, "High performance of a non-polar AlGaN-based DUV-LED with a quaternary superlattice electron blocking layer," *J. Electron. Mater.*, vol. 51, no. 9, pp. 5389–5394, Sep. 2022, doi: 10.1007/s11664-022-09778-2.

[10] G. Zhang et al., "Enhancing the light extraction efficiency for AlGaN-based DUV LEDs with a laterally over-etched p-GaN layer at the top of truncated cones," *Opt. Exp.*, vol. 29, no. 19, pp. 30532–30542, Sep. 2021, doi: 10.1364/OE.435302.

[11] M. Asad, R. Wang, Y.-H. Ra, P. Gavirneni, Z. Mi, and W. S. Wong, "Optically invariant InGaN nanowire light-emitting diodes on flexible substrates under mechanical manipulation," *npj Flexible Electron.*, vol. 3, no. 1, Aug. 2019, doi: 10.1038/s41528-019-0059-z.

[12] S. F. Shiba, J. Y. Tan, and J. Kim, "Multidirectional UV-LED lithography using an array of high-intensity UV-LEDs and tilt-rotational sample holder for 3-D microfabrication," *Micro Nano Syst. Lett.*, vol. 8, no. 1, Dec. 2020, doi: 10.1186/s40486-020-00107-y.

[13] Y. Sang, H. Liu, and A. Umar, "Photocatalysis from UV/Vis to near-infrared light: Towards full solar-light spectrum activity," *ChemCatChem*, vol. 7, no. 4, pp. 559–573, Feb. 2015, doi: 10.1002/cctc.201402812.

[14] B. Rusinque, S. Escobedo, and H. D. Lasa, "Photocatalytic hydrogen production under near-UV using Pd-doped mesoporous TiO_2 and ethanol as organic scavenger," *Catalysts*, vol. 9, no. 1, p. 33, Jan. 2019, doi: 10.3390/catal9010033.

[15] F. Olivier, S. Tirano, L. Dupré, B. Aventurier, C. Largeron, and F. Templier, "Influence of size-reduction on the performances of GaN-based micro-LEDs for display application," *J. Lumin.*, vol. 191, pp. 112–116, Nov. 2017, doi: 10.1016/j.jlumin.2016.09.052.

[16] E. A. Serban et al., "Selective-area growth of single-crystal Wurtzite GaN nanorods on SiO_x/Si(001) substrates by reactive magnetron sputter epitaxy exhibiting single-mode lasing," *Sci. Rep.*, vol. 7, no. 1, p. 12701, Oct. 2017, doi: 10.1038/s41598-017-12702-y.

[17] B. A. Kazanowska et al., "Fabrication and field emission properties of vertical, tapered GaN nanowires etched via phosphoric acid," *Nanotechnology*, vol. 33, no. 3, Oct. 2021, Art. no. 035301, doi: 10.1088/1361-6528/ac2981.

[18] B. Melanson, M. Hartensveld, C. Liu, and J. Zhang, "Demonstration of flexible DUV light emitting diodes through formation of nanowires with inverse-taper," in *Proc. Conf. Lasers Electro-Opt. (CLEO)*, 2021, pp. 1–2.

[19] B. Melanson, D. Starling, M. Hartensveld, G. Howland, S. Preble, and J. Zhang, "Narrow linewidth photoluminescence from top-down fabricated 20 nm InGaN/GaN quantum dots at room temperature," in *Proc. Conf. Lasers Electro-Opt. (CLEO)*, May 2020, pp. 1–2.

[20] B. Melanson, M. Seitz, and J. Zhang, "Inverse tapered AlGaN micropillar and nanowire LEDs for improved light extraction efficiency at 270 nm," *IEEE Photon. J.*, vol. 14, no. 6, pp. 1–10, Dec. 2022, doi: 10.1109/JPHOT.2022.3221353.

[21] B. Melanson, M. Hartensveld, C. Liu, and J. Zhang, "Realization of electrically driven AlGaN micropillar array deep-ultraviolet light emitting diodes at 286 nm," *AIP Adv.*, vol. 11, no. 9, Sep. 2021, Art. no. 095005, doi: 10.1063/5.0061381.

[22] M. Hartensveld, G. Ouin, C. Liu, and J. Zhang, "Effect of KOH passivation for top-down fabricated InGaN nanowire light emitting diodes," *J. Appl. Phys.*, vol. 126, no. 18, Nov. 2019, Art. no. 183102, doi: 10.1063/1.5123171.

[23] M. Hartensveld, B. Melanson, C. Liu, and J. Zhang, "AlGaN nanowires with inverse taper for flexible DUV emitters," *J. Phys., Photon.*, vol. 3, no. 2, Apr. 2021, Art. no. 024016.

[24] S. J. Pearton, H. Cho, F. Ren, J.-I. Chyi, J. Han, and R. G. Wilson, "Properties and effects of hydrogen in GaN," *MRS Internet J. Nitride Semicond. Res.*, vol. 5, no. S1, pp. 540–550, 2000, doi: 10.1557/S1092578300004749.

[25] S. Nakamura, T. Mukai, M. S. M. Senoh, and N. I. N. Iwasa, "Thermal annealing effects on p-type Mg-doped GaN films," *Jpn. J. Appl. Phys.*, vol. 31, no. 2B, p. L139, Feb. 1992, doi: 10.1143/JJAP.31.L139.

[26] A. Papamichail et al., "Mg-doping and free-hole properties of hot-wall MOCVD GaN," *J. Appl. Phys.*, vol. 131, no. 18, May 2022, Art. no. 185704, doi: 10.1063/5.0089406.

[27] A. V. Mazalov, D. R. Sabitov, V. A. Kureshov, A. A. Padalitsa, A. A. Marmalyuk, and R. K. Akchurin, "Research of acceptor impurity thermal activation in GaN: Mg epitaxial layers," *Modern Electron. Mater.*, vol. 2, no. 2, pp. 45–47, Jun. 2016, doi: 10.1016/j.moem.2016.09.003.

[28] J. Chen and W. D. Brewer, "Ohmic contacts on p-GaN," *Adv. Electron. Mater.*, vol. 1, no. 8, Aug. 2015, Art. no. 1500113, doi: 10.1002/aelm.201500113.

[29] Q. Z. Liu and S. S. Lau, "A review of the metal-GaN contact technology," *Solid-State Electron.*, vol. 42, no. 5, pp. 677–691, May 1998, doi: 10.1016/S0038-1101(98)00099-9.

[30] H. Yu et al., "AlGaN-based deep ultraviolet micro-LED emitting at 275 nm," *Opt. Lett.*, vol. 46, no. 13, pp. 3271–3274, May 2021.

[31] H. W. Choi, C. W. Jeon, M. D. Dawson, P. R. Edwards, and R. W. Martin, "Efficient GaN-based micro-LED arrays," *MRS Proc.*, vol. 743, no. 28, pp. 433–438, 2002, doi: 10.1557/PROC-743-L6.28.

[32] R. Koester et al., "High-speed GaN/GaInN nanowire array light-emitting diode on silicon(111)," *Nano Lett.*, vol. 15, no. 4, pp. 2318–2323, Apr. 2015, doi: 10.1021/nl504447j.

[33] F. Yu et al., "GaN nanowire arrays with nonpolar sidewalls for vertically integrated field-effect transistors," *Nanotechnology*, vol. 28, no. 9, Mar. 2017, Art. no. 095206, doi: 10.1088/1361-6528/aa57b6.

[34] M. F. Fatahilah et al., "Top-down GaN nanowire transistors with nearly zero gate hysteresis for parallel vertical electronics," *Sci. Rep.*, vol. 9, no. 1, Jul. 2019, doi: 10.1038/s41598-019-46186-9.
[35] L.-C. Chen et al., "Oxidized Ni/Pt and Ni/Au ohmic contacts to p-type GaN," *Appl. Phys. Lett.*, vol. 76, no. 25, pp. 3703–3705, Jun. 2000, doi: 10.1063/1.126755.
[36] C. Mauduit et al., "Importance of layer distribution in Ni and Au based ohmic contacts to p-type GaN," *Microelectron. Eng.*, vol. 277, May 2023, Art. no. 112020, doi: 10.1016/j.mee.2023.112020.
[37] L.-C. Chen et al., "Microstructural investigation of oxidized Ni/Au ohmic contact to p-type GaN," *J. Appl. Phys.*, vol. 86, no. 7, pp. 3826–3832, Oct. 1999, doi: 10.1063/1.371294.
[38] S.-C. Huang et al., "Study of 375 nm ultraviolet InGaN/AlGaN light-emitting diodes with heavily Si-doped GaN transition layer in growth mode, internal quantum efficiency, and device performance," *J. Appl. Phys.*, vol. 110, no. 12, Dec. 2011, Art. no. 123102, doi: 10.1063/1.3669377.
[39] J. M. Smith et al., "Comparison of size-dependent characteristics of blue and green InGaN microLEDs down to 1 μm in diameter," *Appl. Phys. Lett.*, vol. 116, no. 7, Feb. 2020, Art. no. 071102, doi: 10.1063/1.5144819.
[40] D. Priante et al., "Highly uniform ultraviolet—A quantum-confined AlGaN nanowire LEDs on metal/silicon with a TaN interlayer," *Opt. Mater. Exp.*, vol. 7, no. 12, p. 4214, Dec. 2017, doi: 10.1364/OME.7.004214.
[41] B. Janjua et al., "Ultraviolet—A LED based on quantum-disks-in-AlGaN-nanowires—Optimization and device reliability," in *Proc. IEEE Photon. Conf. (IPC)*, Sep. 2018, pp. 1–12, doi: 10.1109/IPCon.2018.8527172.
[42] C. C. Li et al., "Operating behavior of micro-LEDs on a GaN substrate at ultrahigh injection current densities," *Opt. Exp.*, vol. 27, no. 16, p. A1146, Aug. 2019, doi: 10.1364/OE.27.0A1146.

Matthew Seitz (Graduate Student Member, IEEE) received the B.S. degree in physics from the University of Washington, Seattle, USA, in 2018, and the M.S. degree in materials science and engineering from the Rochester Institute of Technology in 2020, where he is currently pursuing the Ph.D. degree with the Dr. Jing Zhang's Research Group. He is conducting research on the development and fabrication of III-Nitride lasers and μLEDs.

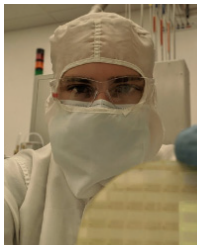

Matthew Hartensveld (Member, IEEE) received the B.S. degree in microelectronic engineering, the M.S. degree in materials science and engineering, and the Ph.D. degree in microsystems engineering from the Rochester Institute of Technology, in 2018, 2018, and 2021, respectively. He is a highly skilled and accomplished semiconductor engineer with expertise in GaN micro-LEDs and transistors. He has a strong background in research and development. He is currently the CTO with Innovation Semiconductor Inc., where he has pioneered the creation of monolithic gallium nitride LED-FETs and innovated color-tunable indium gallium nitride LEDs. He has published 16 scientific articles and pioneering the invention of various semiconductor devices.

Bryan Melanson (Graduate Student Member, IEEE) received the B.S. degree in materials science and engineering with a focus in nanotechnology and nanoengineering from the University of Washington, Seattle, USA, in 2018. He joined Dr. Jing Zhang's Research Group, Rochester Institute of Technology, as a Ph.D. Candidate, in 2018. He is currently conducting research on deep-ultraviolet light emitting diodes and μLED displays, with a focus on improving the light extraction efficiency of these devices.

Jacob Boisvere received the B.S. degree in electrical engineering from Western New England University, Springfield, MA, USA, in 2022. He joined Dr. Jing Zhang's Research Group, Rochester Institute of Technology, in 2023, researching III-Nitride nanostructures.

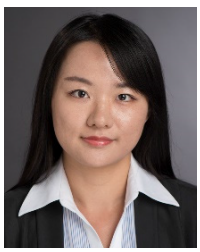

Jing Zhang (Member, IEEE) received the B.S. degree in electronic science and technology from the Huazhong University of Science and Technology in 2009 and the Ph.D. degree in electrical engineering from Lehigh University in 2013. She is currently the Kate Gleason Associate Professor with the Department of Electrical and Microelectronic Engineering, Rochester Institute of Technology. Her research group is working on the development of novel quantum well active regions and substrates for enabling high-performance ultraviolet (UV) and visible LEDs/lasers and engineering of advanced device concepts for nanoelectronics. She has published more than 40 refereed journal articles and 70 conference proceedings, including invited talks. Her research focuses on developing highly efficient III-Nitride and GaO semiconductor based photonic, optoelectronic, and electronic devices. She was a recipient of the Texas Instruments/Douglass Harvey Faculty Development Award and the National Science Foundation (NSF) CAREER Award.